SELF-GENERATED MAGNETIC FIELDS PRODUCED BY LASER BOMBARDMENT OF A SOLID TARGET

Larry Joe Davis

United States
Naval Postgraduate School

THESIS

SELF-GENERATED MAGNETIC FIELDS PRODUCED
BY LASER BOMBARDMENT OF A SOLID TARGET

by

Larry Joe Davis

June 1971

Approved for public release; distribution unlimited.

Self-generated Magnetic Fields Produced by Laser Bombardment of a Solid Target

by

Larry Joe Davis
Captain, United States Army
B.S., Jacksonville State University, 1964

Submitted in partial fulfillment of the
requirements for the degree of

MASTER OF SCIENCE IN PHYSICS

from the

NAVAL POSTGRADUATE SCHOOL
June 1971

ABSTRACT

To investigate the phenomena associated with the production of dense plasmas through solid target bombardment by focused laser radiation, procedures relevant to assembly and operation of a high power giant pulse laser system, laser monitoring techniques, and the experimental arrangement for investigating the properties of a freely expanding plasma were developed.

Using magnetic coil probes in the vicinity of the expanding laser-created plasma, signals were detected which indicated the presence of azimuthal magnetic fields. The magnitudes of the observed magnetic fields were as high as 35 Gauss. The dependencies of the self-generated magnetic fields (SGMF) upon background gas pressure, probe position, and applied external fields were investigated.

A discussion of possible generation mechanisms in light of the experimental evidence is included.

TABLE OF CONTENTS

LIST OF ILLUSTRATIONS

ACKNOWLEDGMENT

Of the many people who have supported this project, I wish especially to thank Mr. Hal Herreman for his enthusiastic assistance in the laboratory, Mr. Michael O'Dea and his crew for flawless and expeditious machining and Professor Fred Schwirzke for his infinite patience.

I also wish to thank the Air Force Office of Scientific Research through whose funding this experiment was made possible.

Research sponsored by the Air Force Office of Scientific Research, Office of Aerospace Research, United States Air Force, under AFOSR Grant No. MIPR-0004-69.

I. INTRODUCTION

The matter discussed in this treatise is the result of the second in a continuing program of experiments to study the characteristic phenomena associated with a laser-produced plasma both with and without externally applied confining magnetic fields. The investigation described herein consisted of the assembly and refinement of the KORAD K-1500 Q-switched laser system and its subsequent use in producing a dense energetic plasma through bombardment of a MYLAR^{TM} film target with the focused beam. The free expansion case was investigated exclusively.

With magnetic coil probes placed in the general vicinity of the laser beam focal spot on the polyethylene film target, signals were recorded which indicated that self-magnetic fields were generated by the expanding plasma cloud. The implications that these self-generated magnetic fields (SGMF), if produced in sufficient magnitude, could be utilized to enhance laser-induced plasma confinement presented themselves. The phenomenon was also conceived to have possibilities as a laboratory model for studying magnetic field generation by various stellar objects as well as solar wind interactions; particularily the magnetopause. A few associated experimental parameters have been investigated and are presented in this thesis; however, extensive improvements to the experimental apparatus became necessary in order to achieve optimum results.

This work is continuing and shall lead to more thorough studies of the SGMF phenomena at the Plasma Physics Laboratory of the Naval Postgraduate School.

II. LASER PRODUCED PLASMAS: BACKGROUND

A. GENERAL THEORY

It would be advantageous to begin with a simplistic qualitative overview of the process of producing plasmas by laser irradiation. Demtröder and Jantz [Ref. 1] have described very graphically an idealized picture of the generation, heating and decay of laser-induced plasmas. This description coupled with the equations developed by John Dawson [Ref.2] provided a solid basis for studying the phenomena associated with the free-expanding laser-induced plasma in the absence of externally applied electric and/or magnetic fields.

In a more specific vein, Afanas'ev and Krokhin [Ref. 3] have considered theoretically the process of vaporization of matter exposed to laser irradiation. Their analysis shows that in the case of transparent material two gas-dynamic modes of vaporization and heating of the solid material are possible. The first mode corresponds to low flux densities when the temperature of the radiation absorbing layer of condensed matter is below a critical temperature and a phase transformation of condensed matter to gas takes place. The second mode relates to fluxes capable of transforming condensed matter into gas by expansion due to thermal pressures. Papers by Fader [Ref. 4], Steinhauer and Ahlstrom [Ref. 5] and Dawson, et al, [Ref. 6] have treated analytically the heating, optical absorption, and expansion of laser-produced plasmas. The

processes associated with the production of overdense plasmas by laser irradiation have been, due to the efforts of the above cited authors among others, to a large degree explained, and many experimental verifications have been made to substantiate the underlying theories. For many years since the advent of high power lasers capable of plasma production from solid targets, the plasma was seen to behave in consonance with most theoretical expectations with some notable exceptions. The relevent exceptions shall be noted in the discussion of the possible generation mechanisms in Section V and in Section B below.

B. SELF-GENERATED MAGNETIC FIELDS (SGMF)

In 1966, Korobkin and Serov [Ref.7] reported upon an investigation into the magnetic field of a spark produced by focusing laser radiation. These investigators used a Q-switched ruby laser with an energy output of 2J and pulse-width of 30 nsec and a lens of 5 cm focal length to create a breakdown in air in the vicinity of the focal spot. With two magnetic coil probes, signals were obtained which were attributed to be due to a change of magnetic flux through the area subtended by the coils. The conclusion was made that a magnetic dipole moment existed within the spark and that this moment was oriented perpendicular to the laser beam propagation direction. The magnetic moment was measured to be approximately (3-5) oersteds/cm^3. The report also asserted that the azimuthal direction of these magnetic moments could be altered by allowing the laser pulse to pass through different portions of the focusing lens. The

authors assumed that the magnetic moments were produced due to the turning of the shock-wave front toward the focusing lens and that this could be due to distortions in the ray caustic and inhomogeneity of the angular distribution of the laser radiation.

In 1967, Askar'yan, et al, [Ref. 8] reported upon the currents produced by light pressure upon a solid target and the expanding plasma cloud. Again using magnetic coil probes, signals were detected which indicated that magnetic dipoles were created in the solid target by currents induced by the electromagnetic interaction with the target surface. This interaction is explained by the authors as due to the influence of light pressure for which an equivalent, non-potential action field can be defined which in turn is equivalent to the action of an electromotive force that pumps electrons through the volume where the light pressure is localized and produces a system of closed currents. The signals in the metal target were seen to reverse when the target was rotated by 45^{o}. Using a double laser pulse mode wherein the two successive laser pulses were separated by approximately 240 ns, a signal was also detected presumably due to the interaction of the second pulse with the plasma flare formed by the first pulse. The signals due to the second laser pulse were larger by one order of magnitude over those produced by the first pulse. It was found that the signal due to the second pulse could be reversed by changing the rotation direction of the Q-switching prism used in the experiment. This procedure

introduces an inhomogeneity into the laser pulse since lasing action is initiated in a system such as this before the Q-switching prism becomes perpendicular to the laser optical axis; therefore, the edge of the laser pulse corresponding to the direction from which the prism is introduced into the optical cavity shall always lead the remainder of the laser pulse front. The generation of these magnetic dipoles were attributed by the authors to be due to current loops formed in the solid target and in the plasma by the interaction of the electric fields associated with the incident laser pulse and the matter of the target and the plasma cloud.

It must be noted that the magnitudes of the fields observed were very small and the time duration of the fields were equal to or shorter than the laser pulse width in both of the above cited reports. Also in both experiments the magnetic moments were oriented perpendicular to the laser propagation direction yielding azimuthal magnetic fields.

In late 1970, Stamper, et al, [Ref. 9] at the Naval Research Laboratories, while investigating the expulsion of an externally applied longitudinal (axial) magnetic field from the expanding plasma cloud, found that self-magnetic fields were being produced by the expanding plasma. These fields as in the previously cited studies were measured using magnetic coil probes placed in the path of the expanding plasma. The magnitudes of these magnetic fields were as high as 1200 Gauss and were primarily azimuthal with reference to the laser beam axis. The plasma was produced by bombarding Lucite fibers of approximately 100 μ diameter with the focused beam of a

high brightness laser with an energy output of 60 J and pulse-width of 30 nsec. The magnetic fields were found to propagate with a velocity approximately equal to that of the luminous and density fronts of the plasma. At probe positions on line with the focal spot on the Lucite fiber but displaced radially, axial magnetic field components were measured, the magnitudes of which were comparable to the azimuthal magnetic field components. Using planar targets of Aluminum and Silver, only azimuthal components were observed and the direction of the signals indicated that axial conventional currents flowed in the direction of the incident laser beam. The magnitudes of the fields were found to be insensitive to background pressure. The observed probe signals had a relatively long duration and a typical signal was approximately 400 nsec in length. The authors attributed the generation of the magnetic fields to currents induced via the thermoelectric effect where the focal spot is considered to form a hot thermoelectric junction.

C. LASER REQUIREMENTS

It was obvious that a high brightness Q-switched laser system was a prerequisite in order to pursue the study of laser-produced plasmas and, in particular, the SGMF phenomena. An important aspect in the production of laser-induced plasmas is that maximum plasma temperatures are attained when the laser pulse is as short as possible. This allows maximum heating to take place before expansion is initiated. It was also recognized that the most interesting phenomena associated

with laser interaction with plasmas occurred at high power density thresholds. These phenomena include but are not limited to affects associated with pondermotive forces, anomalous heating, generation of plasma waves, and onset of multi-stream instabilities. To fulfill interim requirements and to provide a means of later improvements, the KORAD K-1500 Q-switched oscillator-amplifier laser system was purchased. This system is particularly advantageous since manifold increases in the output power was and is capable of being attained by adding additional amplifier units to the existing configuration.

II. LASER ASSEMBLY AND OPERATION

A. K-1Q LASER SYSTEM

The basic component of the K-1500 laser system used in this experiment is the KORAD K-1Q Q-spoiled laser retrofitted for neodymium-glass lasing rod application. The major components of the K-1Q are the K-QS2 Pockels Cell assembly with associated shutter electronics, the K-1 Laser Head with flashlamp power supply, the external Brewster stack polarizer, and the front and rear reflectors. The K-1Q laser functions as the oscillator (or precursor to the amplified giant pulse) in the K-1500 system, therefore optimum pulse output conditions had to be achieved in the K-1Q before proceeding with the K-1500 assembly.

The K-QS2 Pockels Cell Assembly functions as the electro-optical shutter. The KDP (Potassium Dihydrogen Phosphate) crystal is the functional unit of the Pockels Cell assembly. The KDP crystal is affixed between two windows each of which are peculiar to the type of lasing material utilized and is immersed in a dielectric fluid which in addition to preventing high voltage breakdown (since up to 40 KV may be applied to the KDP crystal to attain a proper bias) also provides refractive index matching with the enclosure windows. The windows are each marked on the edge for a 1.06 micron (Neodymium) use and must be mounted with the sides with a non-reflective coating applied facing outward from the crystal. The KDP

crystal is hydroscopic and extreme care must be exercised when replacing window assemblies so that moisture does not contact the crystal. The quartz rear reflector is also mounted on the Pockels Cell assembly and it too is peculiar to the particular lasting material used and must be mounted with the reflective-coating side facing toward the KDP crystal. The principle of operation of the K-QS2 Pockels Cell is based upon the half-wave retardation effect produced due to the birefringence of the KDP crystal. The functioning of the electro-optical shutter is dependent upon the requirement that light of unidirectional polarization be incident upon the KDP crystal. Ruby laser rods fluoresce with a preferred polarization but neodymium-glass rods fluoresce with random polarization. To overcome this difficulty an external polarizer (Brewster stack) is positioned between the neodymium-glass rod and the Pockels cell. The external polarizer must be positioned such that the preferred plane of transmission is normal to the preferred plane of transmission of the Brewster stack between the KDP crystal and the rear reflector. (Only radiation polarized with the electric vector in a direction parallel to the plane of incidence will be preferentially transmitted through the Brewster stack polarizers). When high voltages are placed upon the circular anodes on the end faces of the KDP crystal, it becomes birefringent and with proper biasing and orientation will effectively rotate the direction of polarization of incident light by 90° on each pass through the crystal. The electro-optical shutter may be explained as

follows: Randomly polarized fluorescence radiation is incident upon the external Brewster stack polarizer and only that component with the electric vector oriented in the plane of incidence is transmitted. With the KDP crystal unbiased the radiation will be transmitted unchanged. However, this direction of polarization is not preferred by the rear polarizer stack and the light is reflected from the cavity before reaching the rear reflector. With the KDP crystal properly biased, the polarization of the radiation transmitted by the external polarizer will be effectively rotated 90° to the plane preferred by the rear polarizer stack. The radiation is thereby transmitted to the rear reflector where practically 100% reflection takes place. The returning beam is again "rotated" 90° by the KDP crystal into the preferred transmission plane of the external polarizer allowing the radiation to reenter the laser rod, thereby completing the feedback required for stimulated emission by the laser rod. The biasing voltage for the KDP crystal is furnished by the shutter electronics assembly which delivers a pulse with a maximum amplitude of 50 KV and is characterized by a 10 nsec rise time and 2.5 μsec decay time. The rise time of the bias voltage imposes an absolute minimum of 10 nsec pulse width on the emitted giant pulse. Optimum KDP bias voltage has been found to be #7 on the voltage control vernier for neodymium rod application. This converts to approximately 28 KV.

The addition of the K-1 laser head and the front reflector complete the optical cavity components of the K-10 system.

The front reflector may be utilized with either ruby or neodymium laser rods. The K-1 laser head contains the neodymium-glass rod (1/2" in diameter) surrounded by a UV shield (Pyrex glass tubing) and a spiral flashlamp. The flashlamp is enclosed by an aluminum shield which reflects otherwise errant flashlamp radiation into the laser rod. Extreme care must be exercised in assembling the K-1 laser head to insure that the flashlamp ground connector wire is positioned such that contact with the aluminum reflecting shield is not made during the firing process. If the shield becomes grounded a discharge may occur across the flashlamp envelope resulting in flashlamp explosion. The K-1 flashlamp is fired by discharging a 400 μf capacitor, which may be energized to a maximum of 5 KV by the K-1 power supply, across the Xenon tube. The UV shield is necessary to minimize the absorption of short wavelength radiation by the rod in order to prevent internal damage (solarization). The tubular glass shield also functions as a channel for cooling water flow.

Before aligning the K-1Q system, all components must be positioned upon the optical bench as shown in Fig. 1 in such a manner as to minimize the cavity length (distance from front to rear reflectors). The minimum practical cavity length is approximately 22.5 inches. The following procedure has been found to be the most efficient in the optical alignment of the K-1Q laser system. First, remove the external polarizer from the cavity. Place a small sheet of Polaroid material with the opaque axis vertical between the KDP crystal and

the rear Brewster stack, and another sheet of Polaroid material with the opaque axis horizontal between the KDP crystal and the K-1 head. (The opaque axis of the Polaroid sheets may be readily determined by viewing any illuminated object through both the material in question and the external polarizer.) Illuminate the cavity by placing a uniform white light source at the rear reflector. Position the KORAD miniautocollimator three to six inches forward of the front reflector on the axis of the laser rod. The miniautocollimater is properly positioned when the return dot from the laser rod face is centered upon the eyepiece cross-hairs. Adjust the Pockels cell mounting screws until a shadow in the form of a Maltese cross is centered in the miniautocollimator eyepiece. With this "cross" centered the parallel ends of the KDP crystal are also parallel to the ends of the laser rod. Three return dot images should be visible in the miniautocollimator when viewing along the non-aligned cavity. These return images are due to the two reflections and the front face of the neodymium-glass rod. (A schematic illustrating the operation of the miniautocollimator is shown in Fig. 2.) The optical alignment is completed when by adjusting the rear and front reflector mounting assemblies, the three return dots are made to coincide. The return dot image from the rear reflector is of very low intensity making a darkened surrounding more conducive to accurate alignment. If properly aligned, the K-1Q should operate in the normal mode at this point. The threshold lamp discharge voltage was found to be ~3.85 KV for

the Owens-Illinois lasing material used in this experiment.

To attain giant pulse output the external polarizer must be replaced in the cavity at the proper orientation. To accomplish this the external polarizer is placed into the cavity such that its preferred plane of polarization is approximately normal to the preferred plane of the rear Brewster stack. Place a blackened Polaroid print forward of the front reflector and with the Pockels cell power supply off fire the K-1Q at just above threshold voltage. If a "burn" appears, the external polarizer is improperly oriented. Rotate the polarizer in its mount until no "burn" appears. The K-1Q is thereby made capable of Q-switched giant pulse operation. Using the laser monitoring devices, which are described in section IIID, the K-1Q laser output is optimized by varying the three system parameters; 1) Pockels cell bias voltage, 2) the Pockels cell bias voltage delay time, and 3) the flashlamp discharge voltage. Of the three system parameters, the Pockels cell bias voltage delay time is the most important in optimizing output pulse shape and power. The shutter electronics assembly is capable of delaying the application of the Pockels cell bias voltage from 100 μsec to 3 millisec subsequent to the initiation of the flashlamp discharge. A current rate coil (terminal J5 on the K-1 power supply) triggers the shutter electronics time delay base. The object is to allow maximum population inversion to be attained in the lasing material before closing the electro-optical shutter. The optimum delay time was determined to be 0.74 millisec for the

neodymium-glass rod used. It was found that the Pockels cell bias voltage must be increased gradually as the cumulative number of firings increased. At the time of this writing a delay time of 0.80 millisec is being used.

The output characteristics given in Table 1 were obtained for a flashlamp discharge voltage of 4.15 KV. A typical giant pulse waveform is shown in Fig. 3. Power outputs attained for lamp voltages of 5 KV were approximately 100 Mw but these were deemed to be excessive for the ultimate application to the K-1500 amplifier system when focusing effects by the expansion optics could cause internal damage to the K-1Q laser rod.

TABLE 1. K-1Q Output Characteristics

Pulsewidth (at half-maximum power)	20 ns
Energy	1.25J
Power	62 Mw
Peak Intensity	49 Mw/cm^2
Beam Divergence ($\frac{1}{2}<$, $\frac{1}{2}$ power)	1.5 mrad
Line Width	0.4 Å
Wavelength	1.06 micron
Efficiency	0.15%

The K-1Q laser was found to be reproducable in power output within about two percent from shot to shot with negligible variance in pulse width.

B. K-1500 LASER SYSTEM

The K-1500 oscillator amplifier giant pulse laser system (Fig. 1) is composed of the K-1Q laser described previously in addition to the KORAD K-2 laser head with associated flash-lamp firing electronics, beam expansion optics, and a fire signal delay circuit. Expansion optics are required to expand and collimate the K-1Q (oscillator) pulse to coincide with the larger diameter K-2 (amplifier)rod. In addition a coupling fire signal delay circuit is required to synchronize the arrival time of the K-1Q pulse at the K-2 head when maximum population inversion has been attained in the K-2 lasing material. The K-2 head and associated assemblies are integrated into the K-1Q system as shown in Fig. 4.

The K-2 laser rod (also Neodymium-glass) is 9.5 inches long and has a diameter of 3/4". The output end is cut at the Brewster angle to prevent premature oscillations by the amplifier rod. This is a critical consideration in the use of amplifier rods due to the fact that if the amplifier rod forms its own partial cavity, significant energy depletion will occur before the oscillator (driver) pulse reaches the amplifier rod. An alternative solution would be to apply anti-reflection coatings to both ends of a flat-flat amplifier rod. The amplifier rod must be rotated properly to give the desired direction for the output pulse. The output direction is inclined from the laser system axis toward the long side of the amplifier rod by approximately 30°. There are certain considerations which the K-2 laser head imposes upon the

K-1500 system which are worthy of note. First, the high voltage anode end of the K-2 flashlamp is immersed in a reservoir of a dielectric fluid, Fluorinert^{TM}. This fluid is depleted relatively rapidly and must be replenished after each fifty or so shots to prevent flashlamp failure, and secondly, due to the fact that the K-2 operates at high flashlamp energies (up to 20 KJ), the cooling water (distilled) must be as pure as possible and the ambient water temperature should be maintained well below room temperature. Failure to observe these precautions will result in significant deposits of water impurities on the surface of the laser rod leading to decreased absorption of flashlamp light and a proportionally decreased power output, and the instigation of radial temperature gradients in the rod which can lead to structural failure and a lens effect which affects the output beam divergence [Ref. 10]. The temperature of the cooling water is maintained normally through heat exchange with laboratory tap water, however, on warm days an ice tank must be immersed in the coolant reservoir to maintain low temperatures. Extensive modifications were performed upon the K-2 laser head to improve the reliability of the production model. These modifications shall be discussed in Section C below.

The expansion optics for the K-1500 system consists of two lens - one negative (expanding) and one positive (collimating). The negative lens is placed directly in front of the K-1Q output reflector and is designed to expand the K-1Q pulse by a ratio of 3 to 1 in cross-section at the

positive lens. This ratio is excessive for maximum power output from the K-1500 system since only about 20% of the driving pulse energy is coupled into the amplifier rod. A set of expanding optics providing a 3 to 2 expansion ratio has been ordered but were not used in the work described in this paper. The positive lens simply recollimates the expanded beam so that the oscillator pulse traverses the amplifier rod parallel to its axis. The two lens must be exactly 29.4 cm apart to achieve a truly collimated entrance beam for the K-2 amplifier rod. The most reliable method of achieving the proper separation is to view back toward the K-1Q with the miniautocollimator and slide the positive lens back and forth until the return dot from the front reflector is best focused. The two lens mounts are adjustable so that the output pulse from the K-1Q may be centered upon the input end of the amplifier rod. The beam is moved opposite to the direction the negative lens is moved in the mount. Movement of the positive lens moves the beam in the same direction. The adjustment may be reliably accomplished by mounting a blackened Polaroid print on the input side of the K-2 head and observing the burn pattern produced by the oscillator pulse firing onto an outline of the entrance port.

The fire signal delay circuit (Fig. 5) was constructed by Lawrence Schadegg [Ref. 11] in preliminary work on the K-1500 laser system. It is designed to produce the flashlamp fire signal for the K-1Q oscillator at a variable time after the K-2 amplifier fire signal is initiated. The original

circuit was designed to support two amplifiers; however, the circuit has been modified to provide a wider range of delay times for delayed output #2 and eliminates the delay control for delayed output #1. Both delay control #1 and delay control #2 are functional for one output terminal only - delay output #2. Table 2 gives the ranges of delay times available from the circuit.

TABLE 2. Fire Signal Delay Control

Position	Delay Control 1 Delay Time	Delay Control 2 Delay time
Full Clockwise	0.2 ms	0.2 ms
Full Counterclockwise	0.05 ms	2.1 ms

A delay time of approximately 0.2 millisec was found to provide optimum power output from the amplifier rod, however the output was not significantly affected in a delay time range of from 0.05 millisec to 0.3 millisec.

Using the driving (oscillator) pulse described in Table 1, the K-1500 provided a giant pulse with characteristics provided in Table 3.

Table 3. K-1500 Pulse Characteristics

Flashlamp Voltage	10.0 KV
Energy (Max)	5. 4 J
Pulse - width	10 - 12 nsec
Power	540 Mw
Peak Intensity	230 Mw/cm^2
Beam Cross-section	2.35 cm^2
Efficiency	.027%

Because the K-2 lens rod did not require that a threshold lamp-voltage be established due to the fact that an output reflector was not used, the K-1500 would furnish an amplified pulse at all K-2 lamp voltages above 5 KV. The lamp will not discharge with voltages below 5 KV because of lamp resistance. Throughout the experiment described in section IV below a lamp voltage of 9 KV was predominantly used providing an output power of approximately 330 Mw.

C. MODIFICATIONS

Significant improvements to the operational reliability were made to the K-1500 laser system throughout the laser evaluation phase of the project.

The K-10 oscillator proved to be extremely reliable and required but one modification. The ground terminal connector for the K-1 flashlamp as purchased consisted of a friction sleeve which surrounded the terminal part of the flashlamp.

As the cumulative number of lamp discharges increased the sleeve became loose and eventually dropped off. This was due to the high degree of erosion on the inside surface due to the extremely high currents involved in the lamp discharge. To prevent this failure a simple connector was devised in order to maintain a high pressure smooth connector-post contact. This connector was found to be easily maintained and provided a more reliable connection to ground. The improved connector may be best described as a two part rectangular copper block featuring semi-columlar cuts on adjacent sides to accomodate the flashlamp terminal post and the ground wire. The two blocks could then be joined about the lamp terminal and fastened by common screws on each end of the connector. A set screw as well as solder was introduced into the ground wire well to provide adequate anchorage. A similar connector can be used on the K-2 flashlamp if the occasion arises.

The K-2 laser head proved to be less reliable. The production unit was provided with a Styrofoam flashlamp holder which was molded in a fashion to maximize the flow of cooling water over the rod surface and to provide a secure mounting for the flashlamp. The sharp recoil of the flashlamp during discharged degraded the effectiveness of the mounting material in short order resulting eventually in a broken lamp. A Plexiglas mount was fabricated to provide a more secure mount and to allow finer adjustments of the coolant flow over the rod surface. The inside surface of the holder was lined with foam rubber to provide a cushion for the lamp recoil.

Finally, to provide a greater range of tolerance in the diameter of the laser rod used in the K-2 head, rod mounting plates were fabricated to provide for a less hazardous method of mounting the laser rod. The original mounting plates featured an O-ring water seal seat which surrounded the rubber O-ring on three sides. In order to mount the laser rod it was necessary to force the rod, more or less, into the mounting plate against the O-ring pressure. This resulted in excessive sheer stresses on the end surface of the laser rod, especially the Brewster cut end, and resulted on one occasion in the fracture of the rod face. The improved mounting plates provided for the prepositioning of the laser rod in the plates and of the O-ring in a two-sided seat. Application of a pressure ring provided a good water seal and a rigid mount. Using these mounting plates no pressure was on the rod end surface in the mounting process.

D. LASER MONITORING TECHNIQUES

The K-D1 Photodiode provides a means of monitoring the power and energy outputs of the K-1500 laser on a shot to shot basis when calibrated with an absolute energy measuring device. The K-D1 features a rapid response planar diode and a housing especially designed for pulsed laser applications. Figure 6 shows a typical configuration in utilizing the K-D1 Photodiode to monitor the K-1500 laser output. Approximately four percent of the pulse energy is diverted to the MgO diffuser block which acts as a point source whose intensity attenuates as $1/R^2$. The photodiode is placed an appropriate

distance from the diffuser block to attain a 15-20 volt signal from the power output to a fast rise-time oscilloscope. The pertinent information gained from the pulse power trace are; 1) pulsewidth (at half-maximum amplitude) and 2) pulse shape. Neutral density filters are available for use in the photodiode housing to aid in attaining optimum signal amplitudes. In general, two ND-2 filters are required to achieve best results with the photodiode housing at a distance of 5 inches from the MgO diffuser. The K-1Q pulse wave form shown in Fig. 3 was produced by the K-D1 photodiode. The K-D1 Photodiode energy output produces a negative-going signal the magnitude of which is directly proportional to the energy output in the laser pulse. In the "short" mode, the integrating circuit formed is conducive to faithful integration of 10 ns and shorter power pulses. The energy output is best monitored on a memory oscilloscope. The energy signal requires no special termination at the oscilloscope whereas accurate reproduction of the power signal requires a 50 ohm termination at the scope. Figure 6 shows a typical energy trace.

To accurately monitor the energy output, the maximum energy trace amplitude must be correlated to the actual energy output of the laser. The most direct method of measuring the absolute energy output is through the use of the RN-1 Radiometer. It is designed to trap the beam energy in bundle of fine, insulated copper wire which functions both as a calorimetric mass and as a bolometer element. The change in

resistance of this wire element is proportional to the energy absorbed and is practically independent of the distribution of energy within the unit. The bolometer element is part of a conventional Wheatstone Bridge circuit and the change of balance of the bridge is a measure of the beam energy. A schematic of the RN-1 is shown in Fig. 7. The bolometer element is housed in a cylindrical container with a 1/16 inch thick fused quartz window which transmits about 100% of all radiation from 0.26 to 3.1 microns wavelength. In calibrating the absolute energy output against the K-D1 photodiode energy trace, the bolometer element is placed in the beam directly behind the beam splitter. The bridge imbalance is measured with a micro-millivoltmeter (i.e., Kiethley Model 149). The maximum micro-millivoltmeter deflection is related to the laser energy output by the equation:

$$\left(\begin{array}{l}\text{Observed reading}\\ \text{in milliwatts}\end{array}\right) (1.6) = \left(\begin{array}{l}\text{Laser Output}\\ \text{in Joules}\end{array}\right) \qquad (1)$$

This is only ~96% of the energy since 4% of the beam is diverted to the photodiode by the beam splitter. A straight line calibration curve of absolute energy output versus the maximum amplitude of the photodiode energy output trace may be obtained; the slope of which is the proportionality constant relating the absolute laser energy output to the K-D1 photodiode energy signal amplitude. The configuration of the calibration setup must be maintained in all subsequent work since the position and orientation of the MgO diffuser and the photodiode directly affect the magnitude of the energy

and power output signals. Each change in the geometry of the monitoring setup requires a new calibration.

In order to align the experimental apparatus on the path of the laser beam, a continuous wave helium-neon gas laser was used as a reference. The Cw gas laser was positioned behind the rear reflector of the K-1Q laser and centered upon the axis of the optical components of the K-1500 laser system. This visible beam provided a ready reference to the path of the amplified giant pulse. A slight difficulty arises at the Brewster cut output end of the amplifier rod due to the wavelength difference between the helium-neon light and the longer wavelength neodymium light in the amplified pulse. The Cw beam exits at the Brewster cut end at a slightly larger angle than does the giant pulse. This difference in deflection amounted to about 2 mm at one meter from the output end. This difference is significant when probe positions were close to the beam therefore necessitating careful determination of the relative positions of the two beams at all points of interest along the path.

IV. EXPERIMENTAL PROCEDURE AND RESULTS

A. EXPERIMENTAL CONFIGURATION

Using the K-1500 laser as a source of high brightness light energy, the characteristics of the free-expanding plasma created by bombarding a solid target have been studied. A six-port vacuum chamber (Fig. 8) was utilized to support the target and focusing lens and provided ports for positioning various probes into the vicinity of the target. The chamber was connected via the bottom port to fore and diffusion pumps which provided pressures as low as 10^{-5} Torr in the chamber. The K-1500 laser amplified pulse was focused with a lens of 28 cm focal length. A circular sheet of Mylar (Polyethylene Terephthalate), $C_{10} H_8 O_4$, of 127 micron thickness was suspended from the top port of the vacuum chamber at the focal spot of the lens. The plane of the target was maintained, as nearly as possible, in a position perpendicular to the incident laser beam. The focal spot diameter at the target was approximately 2 mm, however, the burn hole in the Mylar film was about 50% larger due to the fact that the material surrounding the focal spot experienced heating and deflagration due to heat conduction from the focal spot. This resulted in bulk material expulsion from the area surrounding the focal spot. The laser power density incident upon the target was approximately 10^{10} watts/cm^2.

B. ABSORPTION (REFLECTION) CHARACTERISTICS

By positioning the MgO diffuser at the vacuum chamber port opposite the lens (laser input) port and observing the power trace signal from the K-D1 photodiode, a rough determination could be made of the absorption characteristics of the Mylar target. Figures 9a and 9b show the laser pulse traces for the exiting pulse without and with the target in position, respectively. Comparison of the energy output signals indicated that approximately 40% of the laser energy was absorbed by or reflected from the laser-produced plasma over the entire pulse length. It is of interest to note that the two curves follow approximately identical traces until the laser intensity is approximately 60% of the maximum power produced in the pulse. Therefore the Mylar target is essentially transparent to the low intensity radiation at the front of the laser pulse. The on-set of absorption/reflection at the threshold intensity indicates that a solid-plasma phase transition takes place in the material, a process in consonance with the approach taken by Alfanas'ev and Krokhin [Ref. 3]. In general, the assumption can be validly made that the solid-plasma phase transition occurs within the first 1-3 nanoseconds of the laser pulse interaction with the target. No attempts were made to experimentally measure the reflected portion of the incident laser light due to the cumbersome requirements but it is estimated that a negligible portion is actually reflected due to the fact that the plasma rapidly expands forming under-dense absorbing plasma layers.

The radiation emitted in the flare at the focal spot into the solid angle subtended by the MgO diffuser was negligible compared with the transmitted laser radiation and was not considered.

C. BACKGROUND PRESSURE DEPENDENCE

To investigate the self-generated magnetic field, a large (1 cm) diameter magnetic probe with two coil-turns shielded by a metallic sleeve was introduced into the path of the expanding laser-produced plasma on the laser side of the target. No external magnetic field was applied to the system. The probe position was at or near a point in the horizontal plane defined by the incident laser beam. Figure 10 shows the probe orientations referred to in the description of the data. The probe signal was relayed to a fast rise-time oscilloscope (i.e., Tektronix Model 7704) via shielded cable terminated by 50 Ω at the oscilloscope. The oscilloscope trace was initiated by an external trigger pulse taken from the T-out terminal on the shutter electronics unit. This trigger pulse corresponds to the application of the biasing voltage in the Pockels cell. A typical probe signal obtained with the center of the large probe at a distance of ~0.6 cm from the target ($PD_{\parallel}$) and ~0.6 cm ($PD_{\perp}$) from the incident laser beam is shown in Fig. 11a. The probe is oriented in the ($\perp$) position. The signal obtained is proportional to dB/dt. Figure 11b shows the signal obtained under identical conditions with the probe rotated by 180°. The reversal of the signal indicates that it is due to the change in magnetic flux through

the coil and not to electrostatic processes. With the probe oriented in the (||) position no signal was obtained. As a check the target was removed and no signal was obtained with any orientation. Repeated verifications have shown that the signals obtained were in fact due to magnetic effects and that the changing field was an azimuthal field with reference to the laser beam. These signals had singular importance in that the ability of the K-1500 laser to produce the magnetic field effect was established. Using the large probe, $\dot{B}$ signals were recorded with background pressures ranging from $1 \cdot (10^{-5})$ Torr to 350 μ of N_2. Figures 12a, 12b, 12c and 12d show some representative signals for background pressures of $6 \cdot (10^{-4})$ Torr, 1.0 μ, 200 μ and 350 μ, respectively. While the magnitudes of the self-generated B-field remained relatively constant, the time duration (τ) of the signal decreased, in general, as the background pressure was increased. At the higher pressures short high amplitude "spikes" were observed both before and after the $\dot{B}$ signals [Fig. 12d]. These "spikes" are believed to be due to a photoelectric effect or other electrostatic interaction with the probe shielding sleeve and were not observed when a smaller glass-shielded probe was used. However, it must be noted that the response of the small ten-turn magnetic probes used diminished at signal frequencies above 30 MHz. The small probes could not, therefore, be expected to detect these small high frequency (~100 MHz) spikes if they were of magnetic origin.

D. MAGNITUDES OF THE SGMF

Using a small probe of n = ten turns encompassing an area of $6(10^{-3})$ cm^2 [$nA = 6(10^{-2})$ cm^2] and an operational amplifier integrating circuit, the magnitudes of the self-generated magnetic fields were measured as a function of parallel probe distance ($PD_{||}$), and perpendicular probe distance ($PD_{\perp}$). The magnitudes of the magnetic fields were related to the maximum amplitude of the integrated signal by the formula [Ref. 12]

$$B[\text{Gauss}] = 10^8 \frac{V_o[\text{Volts}]\ R[\text{Ohms}]\ C[\text{Farads}]}{nA\ [cm^2]} \qquad (2)$$

A plot of the magnitudes of the SGMF against parallel probe distance is shown in Fig. 13. The perpendicular probe distance was maintained at 0.25 cm and the background pressure was 50 μ N_2 for the measurements shown in Fig. 13. Figure 14 shows the results of magnitude measurements with perpendicular (radial) probe distance. This data was taken with background pressure of 65 μ N_2 and a constant parallel probe position of 0.75 cm. The time duration (τ) of the magnetic field signal is also included for the perpendicular probe distance data to illustrate the diffusive nature of the observed signals. Because of the rapid attenuation of the signal at probe distances greater than 1 cm increments of distance less than ~2 mm were considered unreliable pending the application of a more reliable method of measuring the probe position.

E. EFFECT OF THE EARTH'S FIELD

To inquire into possible mechanisms for generation of the observed magnetic field, an external magnetic field was introduced into the expansion volume with Helmholtz coils. The intention was to simulate the horizontal component of the earth's field in this region and to determine the effect upon the plasma-generated fields. The external field was applied parallel to the plane of the target and perpendicular to the incident laser beam. Using field values ranging from 0 to 43 Gauss, no gross deviation in the magnitudes of the self-generated magnetic fields were observed. Figures 15a, 15b and 15c show integrated traces for 0, 21 and 43 Gauss impressed fields, respectively.

F. PROPAGATION VELOCITY

The propagation velocity of the SGMF was found to be on the order of 10^7 cm/sec. This velocity was arrived at by measuring the time separation from the approximate arrival of the laser pulse at the target to the initiation of the magnetic probe signal. The K-D1 photodiode power signal was taken to represent the laser beam at the target since the optical pathlength from the beam-splitter to the photodiode was approximately equal to the optical pathlength to the target. An optical pathlength difference of 10 cm would only introduce an error of 0.3 nanosec in the expansion time. A schematic of typical oscilloscope traces to determine the expansion velocity of the SGMF is shown in Fig. 16. To gain

some insight into the relative location of the expanding plasma front at the onset of the magnetic probe signal, a single electrostatic probe was introduced into the vacuum chamber at, as nearly as possible, the same location as the magnetic probe. The electrostatic probe was unbiased and was connected to ground through a 50 Ω resistance. The electrostatic probe signal is therefore proportional to the current flowing through the termination resistance due to collected charge on the probe. Figures 17a and 17b show the electrostatic probe signal and the magnetic probe signal, respectively, taken on two successive shots under identical conditions. While it is difficult to ascertain anything qualitative with regard to the single electrostatic probe signal, it does give an approximate interaction time of the expanding plasma front with the probe. The initial sharp spikes in the electrostatic probe trace is believed due to photoionization by the laser beam and photoelectric effects due to the "flare" radiation. It is of interest to note that the time duration of the field is approximately 400 nanosec in both cases.

G. TARGET ORIENTATION

As noted by Dawson, et al [Ref. 6] and confirmed by Stamper, et al [Ref. 9], the laser-produced plasma expands non-isotropically with the greatest expansion velocity occurring normal to a plane target. Throughout the experiment described above the target orientation was of critical concern. In order to obtain useful information, a different

portion of the Mylar film target was of necessity exposed to the focused laser beam for each shot and thereby made it necessary to traverse or rotate the target to accomplish same. This process invariably introduced changes of up to 5^{o} in the angle of incidence of the laser beam upon the target. Shearer [Ref. 13] has found that the amount of reflected laser light is enhanced with oblique incidence. Shearer has shown that the ratio of reflected intensity to incident intensity is given by

$$\frac{I_R}{I_o} = \exp\ [-2p\ \cos^5\ \theta_o] \qquad (3)$$

where p is the optical thickness of the plasma layer from the vacuum to the critical density N_c for laser light at normal incidence and θ_o is the angle between the incident laser beam and the electron density gradient vector. This effect was noted early in the performance of the experiment described above and it was found that reproducable results could be attained only when the target orientation was painstakingly maintained at a constant angle relative to the incident laser beam. This problem could be virtually eliminated by using fibers or pellet-shaped targets. However, accurate positioning of the fiber and/or pellet in the laser focal spot would remain to be of major concern to produce consistent data.

V. DISCUSSION OF POSSIBLE SGMF MECHANISMS

A. CHARACTERISTICS OF SGMF (EXPERIMENTAL)

The magnetic fields observed in this experiment were ostensibly due to mechanisms associated with the formation, heating, and expansion of the plasma produced by an intense ($\sim 10^{10}$ watt/cm^2) laser pulse incident upon a planar solid target (MYLAR). Before discussing possible mechanisms to which the observed fields might be attributed, it would be helpful to review the results obtained in the experimentation described in Section IV. Some experimental evidence to be alluded to later in the discussion, due to the work of other reporting investigators, shall provide greater insight as to specific theories of the magnetic field generation process. A summary of the characteristics associated with the self-generated magnetic fields are:

1) The magnitudes of the SGMF increased as the magnetic probe position approached the laser beam-target juncture.

2) For a constant probe position, the time duration of the magnetic field decreased with increased background gas pressure. Because the onset and cessation of the magnetic probe signal was, in general, well defined, the time duration is taken to be the entire time interval over which the signal was recorded.

3) The point of peak magnetic field magnitude ostensibly propagated at or near the velocity of the plasma front.

4) The magnetic signals became more diffuse as the probe position was displaced away from the "hot spot" on the target and appeared to occupy regions of space approximately equal to the spatial extent of the expanding plasma.

5) The introduction of external magnetic fields to simulate the earth's field in the region of expansion caused no significant changes in the magnitudes of the SGMF.

6) The observed magnetic fields were always in an azimuthal direction. No axial component was detected.

In the experiment conducted by Stamper, et al [Ref. 9] it was possible, by using Lucite fibers as target material, to obtain signals with magnetic probe positions very close to the laser beam-target juncture. At a magnetic coil probe position characterized by $PD_{||} = 0$, it was found that the time duration of the $\dot{B}$ signal was very nearly that of the laser pulse.

B. TURBULENT/SHOCK PROCESSES

The initial production of the over-dense plasma by laser pulse irradiation is at best a catastrophic process. Recognizing that the laser power is delivered to the plasma in a time of 10-15 nanoseconds and that the laser pulse is characterized by inhomogeneties with respect to space and time would lead to the conclusion that strong disturbances created by localized hot spots and anisotropic pressure gradients might be established in the laser-created plasma during the production process. The early investigators, Korobkin and Serov and Askar'yan, et al, [Ref. 7 and Ref. 8, respectively], were able to reverse the directions of the small magnetic moments produced by altering the incident laser pulse, the former by directing the incident laser beam through a different portion of the large focusing lens used, and the latter, by reversing the rotation direction of the Q-switching prism of the laser. Basov, et al [Ref. 14] using shadowgraphic techniques to photograph the expanding plasma flow have shown that the expansion is ostensibly non-turbulent initially and only at

distances large compared with the focal spot dimension and at relatively high residual background gas pressures does the expanding flow exhibit turbulent flow. Due to the high initial plasma pressure due chiefly to particle densities on the order of 10^{20}-10^{21} cm^{-3}, the dominant dynamic process is that of rapid expansion into the regions of low particle pressure and it is not deemed probable that significant perturbations on this overriding directed plasma velocity could be established, especially since the plasma is overdense and collision-dominant. Many theoreticians, notably Vainshtein [Ref. 15] and Moffatt [Ref. 16], have treated the "dynamo" process associated with turbulent flow of conducting fluids. Vainshtein has shown that gyrotropic turbulence, where the density of the probability distribution of the velocities is not invarient under reflections, may generate large-scale magnetic fields whereas anisotropic turbulence which may serve as a model for turbulent connection does not generate large scale fields. Moffatt has shown also that gyrotropic turbulence may create a "dynamo" effect wherein a random superposition of inertial waves in a rotating conducting fluid can systematically transfer energy to a magnetic field which has no source other than electric currents in the fluid. The mathematical formulation presented by the above authors is straightforward but lengthy and not deemed essential in this discussion.

Also of interest are the non-linear forces due to the interaction of the intense laser beam with the dense plasma.

These forces exceed the gas-dynamic forces if the increase of the electrodynamic momentum flux density due to collection effects over the vacuum value is larger than the gas-dynamic power density. Hora and Wilhelm [Ref. 17] have asserted that the non-linear force effect is important if the amplitude of the electric field of the radiation in the vacuum exceeds

$$E^* \equiv \sqrt{\frac{4m_e\omega^2}{e^2} K_\beta T} \tag{4}$$

with m_e = electron mass, ω = cyclic frequency of the laser radiation, K_β = Boltzmanns constant, and T = electron temperature. For neodymium laser radiation this critical electric field corresponds to an intensity of

$$I^* = 9.06\ (10^{12})\ T \text{ watts cm}^{-2} \tag{5}$$

This effect cannot, under the above criteria, play a significant role in the generation of the magnetic fields of Section IV since the laser intensity at the focal spot was at least two orders of magnitude smaller than I^*. These forces as analyzed by Lindl and Kaw [Ref. 18] are directed counter to the direction of the laser radiation, however, except when a standing wave is formed between the boundary and the reflection point ($\nu_p \approx \nu$) at which time the force would produce a "bunching" effect which might result in striations in the expanding plasma. It is not likely that laser beam-plasma interactions of the type described would

generate large scale turbulence or the observed magnetic field.

The interaction with significant momentum coupling of the expanding plasma with the background gas has not been found to play a significant role in the production of the observed magnetic fields as indicated in Section IV; however, the time duration of the SGMF was seen to diminish slightly as the background pressure was increased. This can be explained by recognizing that the background gas is partially ionized by the intense flare radiation emitted by the expanding plasma and by the streaming plasma particles themselves. This in effect "feeds" the plasma and results in increased plasma densities near the front and in the formation of a shock front at the plasma-gas interface. The resultant heating behind the shock diminishes the magnetic viscosity and thereby the diffusion rate of a magnetic field which may be trapped inside the plasma.

Kubo, et al [Ref 19] and Basov, et al [Ref. 20] have investigated in a rather extensive manner the formation of shock fronts in the laser-produced plasma as it expands through residual gas. The gas pressure behind the expanding shock front is given by Ref. 14 as

$$P \approx (1 - \frac{1}{\beta} \rho_1 v_y^2) \qquad (6)$$

where β is the compression, ρ_1 is the density of unpreturbed gas, and v_y is the front velocity. The width of the shock was found to vary in approximately inverse proportion to

background pressure thereby establishing sharp density gradients at the leading edge of the shock. Typical electron density profiles in the shock regime does not indicate order of magnitude changes of electron densities in the shock front. Due to the experimental evidence that the observed SGMF increases as the probe position approaches the laser beam - target juncture, it appears that the observed magnetic fields are generated before the shock front is established and the net effect of the residual gas in the expansion space serves only to complicate the gas-dynamic processes in the expanding plasma. Turbulent processes, if present, would be very difficult to observe before the plasma expansion reaches dimensions large in comparison to the focal spot.

The evidence available thus far does not support a turbulent mechanism for the generation of the observed magnetic field. This evidence is especially typified by the apparent independence of applied external magnetic fields, which would discount the amplification of the earth's field in a "dynamo" mechanism, and of residual gas pressure. The observed fields, within experimental error, were observed to have azimuthal components only, implying axial currents. Random turbulent mechanisms which might initiate surface current loops would invariably establish magnetic moments oriented randomly and contribute axial as well as azimuthal magnetic fields.

C. CURRENT FORMATION

Bosov, et al [Ref. 20] have presented some experimental data which indicate that a space charge is established at

the expanding plasma front. Most interesting is the experimental evidence that the expanding plasma flow emitted electron currents with electron energies greater than 100 eV. This experiment was carried out using laser power outputs of the order of magnitude as that used in the experiment described in Section IV. The time during which the electron emission current decreased by one-half was found to be $2 \cdot (10^{-7})$ sec, the approximate duration of the magnetic probe signals at $PD_{||} > 0$. It must be noted here that Bosov, et al, obtained electrostatic probe signals quite similar to those obtained in the experiment described in Section IV [See Fig. 17a]. The negative going signal was interpreted by the authors to be due to the space charge and the positive going signal as due to the main plasma volume which had become positively charged due to the emission of electrons to the space charge region. In reference to Figs. 17a and 17b, it is of interest to note that if the Bosov interpretation is accepted, the maximum negative signal representing the passage of the region of maximum electron density thus maximum emission current coincides quite well with the maximum magnitude of the SGMF signal ($\dot{B} = 0$). If the emission currents were of thermal nature and emanate from the plasma boundary surface, the emission current I is proportional to the surface area, the electron density, and the average electron velocity, $I \alpha R^2 n_e \langle v_e \rangle$, where the electron density is $n_e \sim R^{-3}$ and the mean electron velocity is $\langle v_e \rangle \sim T^{\frac{1}{2}}$. In the case of spherical adiabatic expansion, $T \sim R^{-2}$, whence $I \sim R^{-2}$

[Ref. 20]. If the self-generated magnetic fields were then due to an "average" line current in the direction of the laser beam perhaps due to the anisotropy of the expansion in the laser beam direction, it should be proportional to R^{-3}. This dependence is not found to be evident in investigation of the SGMF which implies that if in fact the electron current emission does occur it occurs through non-equilibrium processes, such as shock wave formation, for example. The electron emission currents would always be in the direction of the laser beam and therefore does not explain the ostensible field reversing effects described by Korobkin and Serov and the Askar'yan group [Refs. 7 and 8, respectively]. Demtröder and Jantz [Ref. 1] have supported the idea of a space-charge influenced expansion wherein the potential of a metallic target exposed to intense laser irradiation was measured. It was observed that the target remained positively charged for approximately 1.2 microseconds subsequent to the arrival of the laser pulse on the target indicating a greater expulsion of electrons than ions from the target.

Stamper, et al, [Ref. 9] have attemped a quantative explanation of the observed magnetic field generation as due to anisotropicities in the thermoelectric power at the focal spot (laser beam-target juncture). Utilizing the generalized Ohm's Law

$$\vec{J} = \sigma(\vec{E} + \vec{v}_e \times \vec{B}/c + \frac{\text{grad } P_e}{n_e e} - \overleftrightarrow{\alpha} \cdot \text{grad } T) \tag{7}$$

$$= \frac{c}{4\pi} \text{ curl } \vec{B}$$

where $\overleftrightarrow{\alpha}$ is the plasma thermoelectric tensor and P_e, n_e and T are the electron pressure, density and temperature, respectively. Taking the curl of (7) and rearranging

$$\frac{\partial B}{\partial t} = \text{curl } (\vec{V}_e \times \vec{B}) + \frac{c^2}{4\pi\sigma} \nabla^2 \vec{B} + \vec{S}(\vec{r}, t) \quad (8)$$

where σ, the plasma conductivity, is assumed to be scalar, and $\vec{S}(\vec{r}, t)$ are the source terms, i.e., the $\overleftrightarrow{\alpha}\cdot$grad T term and the grad P_e term, if (grad n_e x grad $T_e \neq 0$). The thermoelectric contribution would vanish if $\overleftrightarrow{\alpha}$ were a scalar independent of position, i.e., if there were no discontinuities or junction contacts. The laser beam-target juncture is presumed to represent a discontinuous thermoelectric junction contact and provides a non-vanishing thermoelectric contribution. The solution obtained by Stamper, et al, in spherical coordinates was

$$B_\phi(\rho, t) = \left(\frac{c}{e}\right) (K_\beta T_o / v_o \rho) \, f\left(t - \int_o^\rho d\rho / v_o\right) \quad (9)$$

with the source term assumed to be

$$\vec{S}(\vec{r}, t) = (cK_\beta T_o / e)[\hat{\alpha}(\rho)/\rho] \, f(t) \quad (10)$$

Where T_o is the source electron temperature and f(t) is the shape of the laser pulse in time. It was also assumed that the expansion velocity v_ρ is given by

$$v_\rho = v_o \, U\left(t - \int_o^\rho d\rho / V_o\right) \quad (11)$$

where U is the Heaviside unit step function. The basic

assumption involved in the Stamper mechanism is that the thermoelectric tensor is non-scalar due to the discontinuity at the laser beam-target juncture; the thermoelectric contact. It is felt that the thermoelectric junction may be more aptly described as the plasma reflection point for the laser radiation ($\nu = \nu_\rho$) and that the junction is effectively discontinuous so long as the e-folding length for laser radiation penetration past the reflection point is less than the thermal wavelength for heat conduction into the sublimated target material.

VI. CONCLUSIONS

Of prime importance in this initial work on the self-generated magnetic field phenomena is that the giant pulse created by the K-1500 laser and its subsequent absorption by a Mylar target material is precursory to the generation of magnetic fields exhibiting the general characteristics as those observed in experiments conducted by Stamper, et al. The K-1500 laser system with the utilization of the procedure established in this work and the noted modifications should provide a long term, reliable giant pulse producer to study further aspects of the SGMF.

The question of the mechanisms underlying the generation of the magnetic fields observed in this experiment is by no means clear and a great deal of investigation will be necessary to establish further concrete ideas. At the present time, the generation explanation proposed by Stamper, et al, seems to be plausible, yet it obviously reflects some defects, not the least of which concerns the maintenance of the magnetic fields over times very large compared to the laser pulse width. Clearly a thorough study of the plasma properties at times late in the expansion process are also in order and how these properties affect the SGMF. Also open for examination is the effect that the SGMF will have on the expanding plasma. The shell structure noted by Tuckfield and Schwirzke [Ref. 21] may be attributed directly to

the SGMF effect, to cite an example. It appears that the expanding plasma electrons would also become tied to this field whereas the ions are allowed to stream through relatively unimpeded. A mechanism of this type may tend to cancel or enhance the field due to the establishment of conventional ion currents in the plasma.

Other studies which might be undertaken concern the effect of the SGMF upon the utilization of the laser-produced plasma as a target plasma in neutral beam injection mirror machines [Ref. 22]. Also of current interest is the influence of the SGMF upon the electronic heat conduction and other plasma properties. It is felt that the work described in this treatise establishes a basis for many areas for future endeavors in the study of the phenomena associated with laser-produced plasmas.

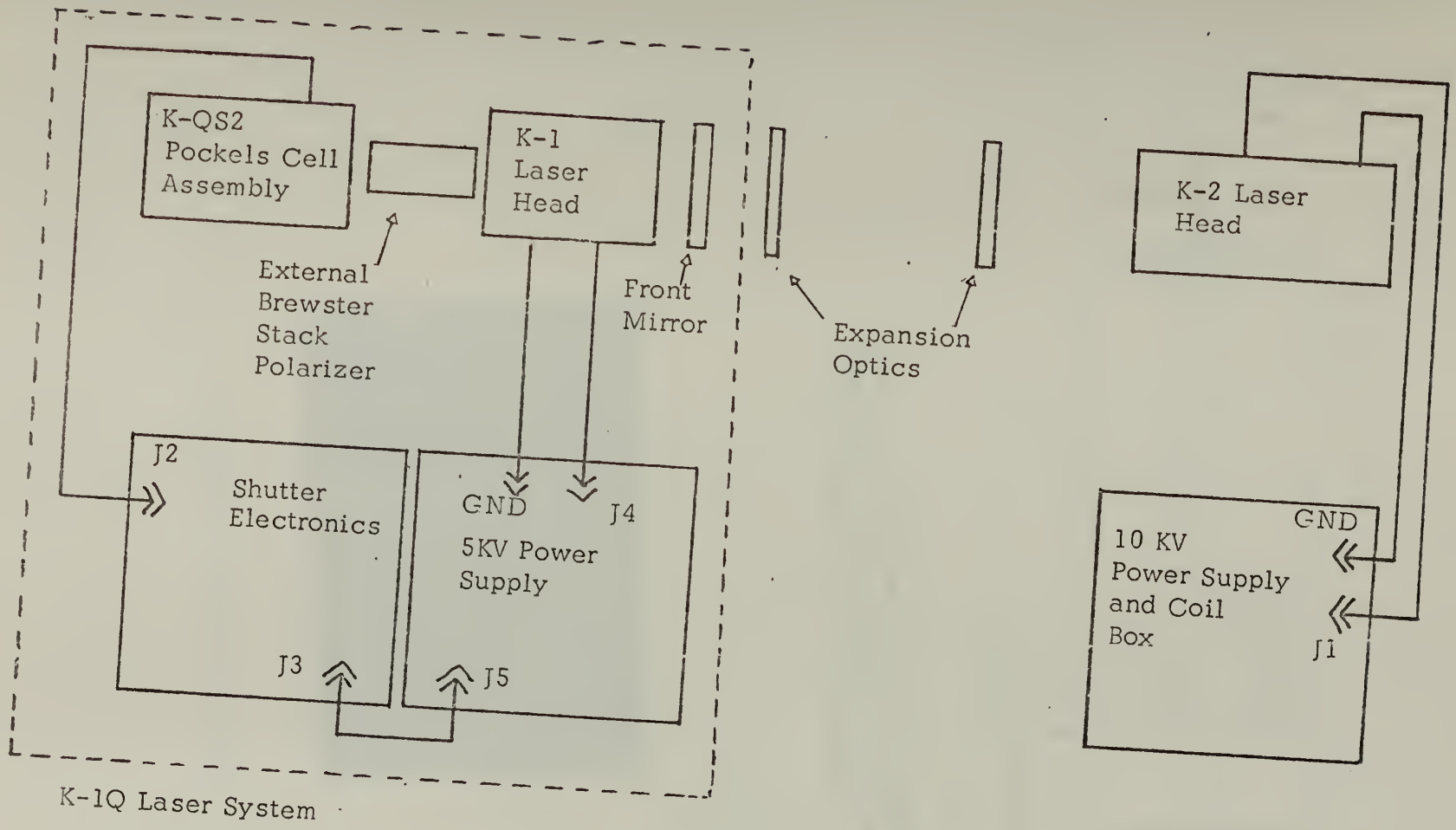

Fig. 1. K-1500 Laser System Set-up. (Water cooling pump w/ connections and fire-signal control assembly omitted)

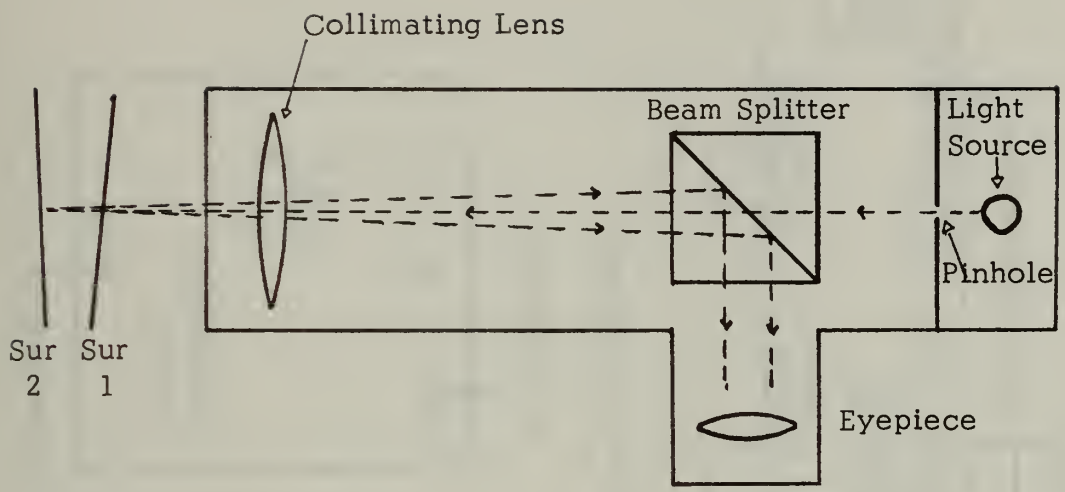

Fig. 2. KORAD Miniautocollimator Schematic. Surface 1 and surface 2 are parallel when return dots are superposed.

Fig. 3. K-1Q Laser Output Waveform. Scale: 20 ns/div.

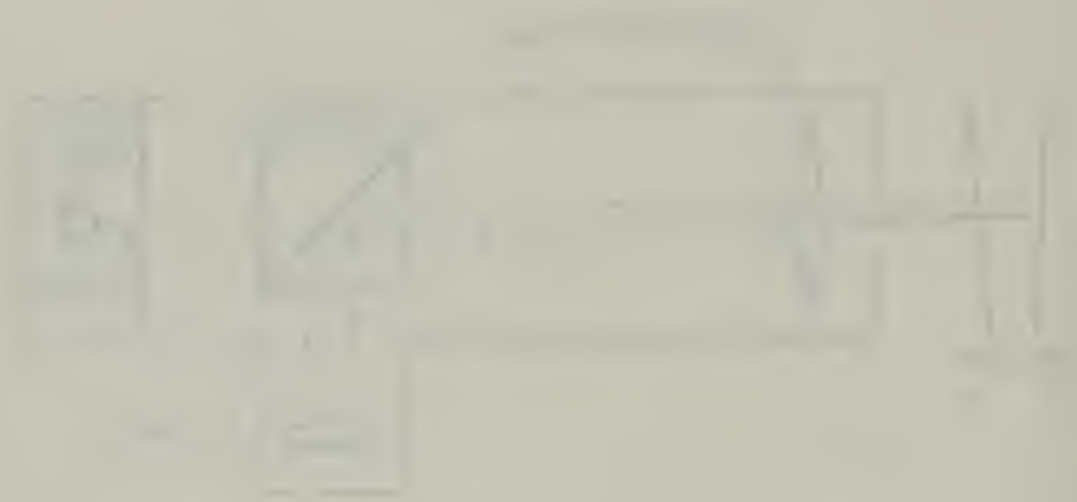

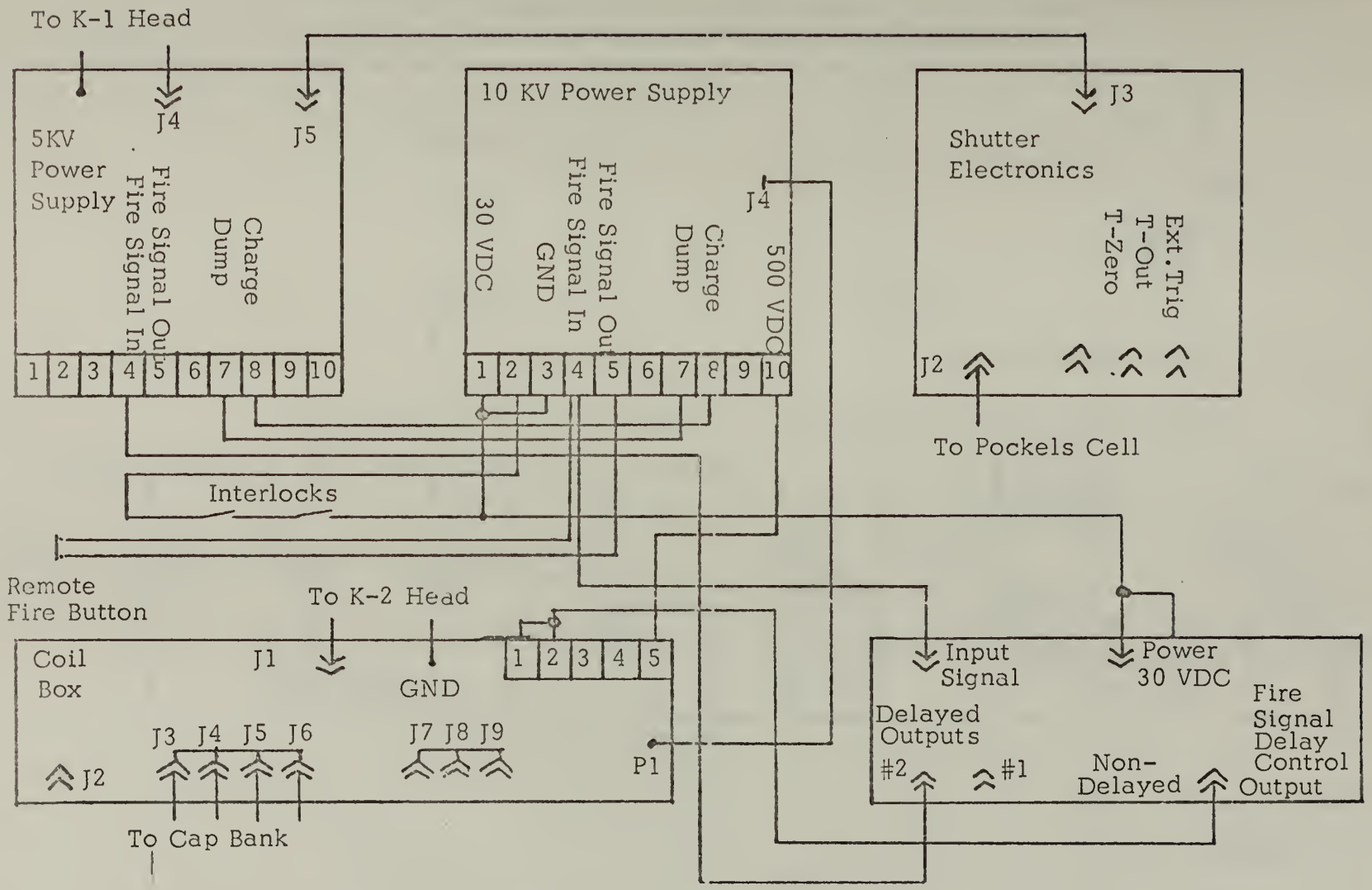

Fig. 4. K-1500 Laser System Circuit Diagram

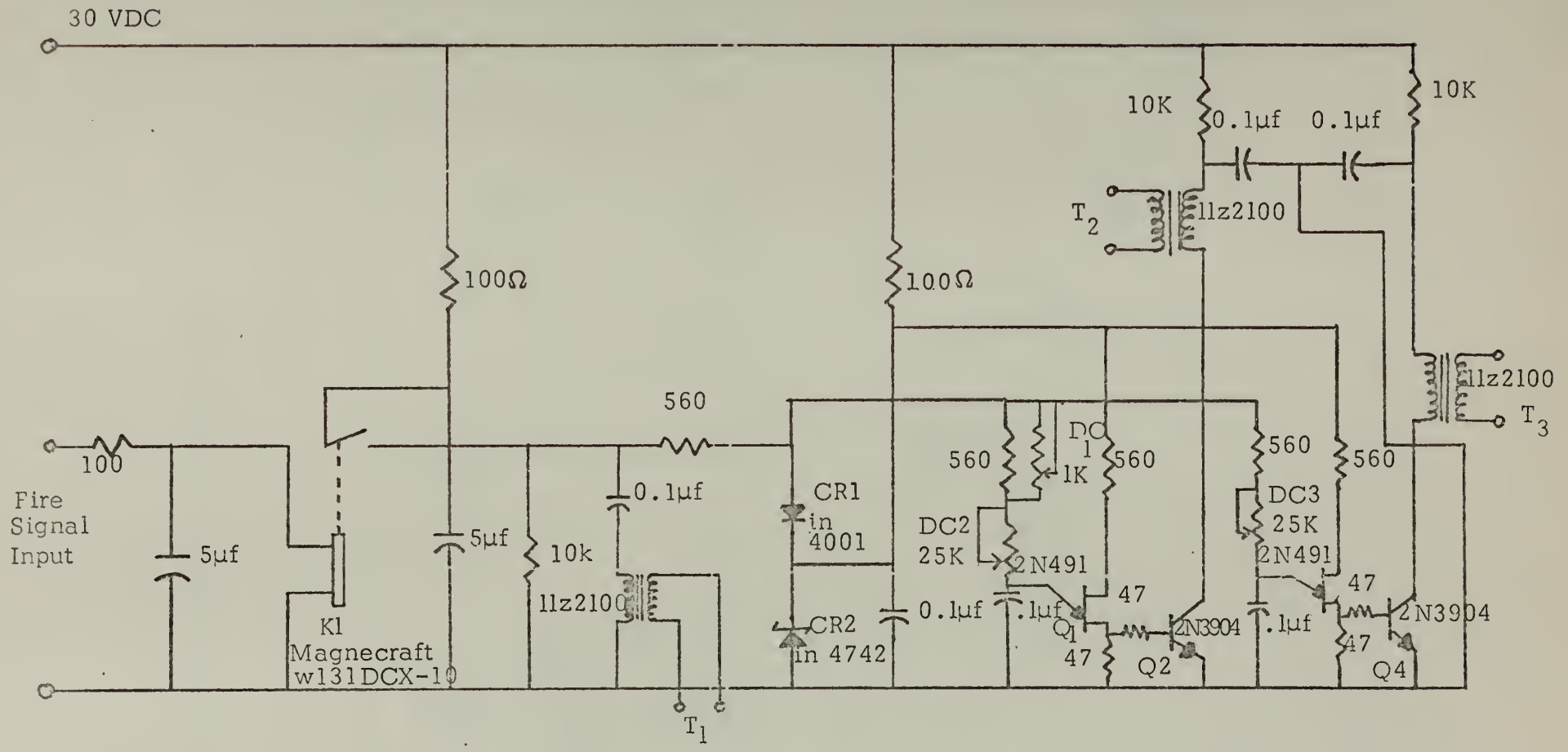

T_1 - Nondelayed Output

$T_{2,3}$ - Delayed Output

DC = Delay Control Pot

Fig. 5. Fire Signal Delay Control Circuit

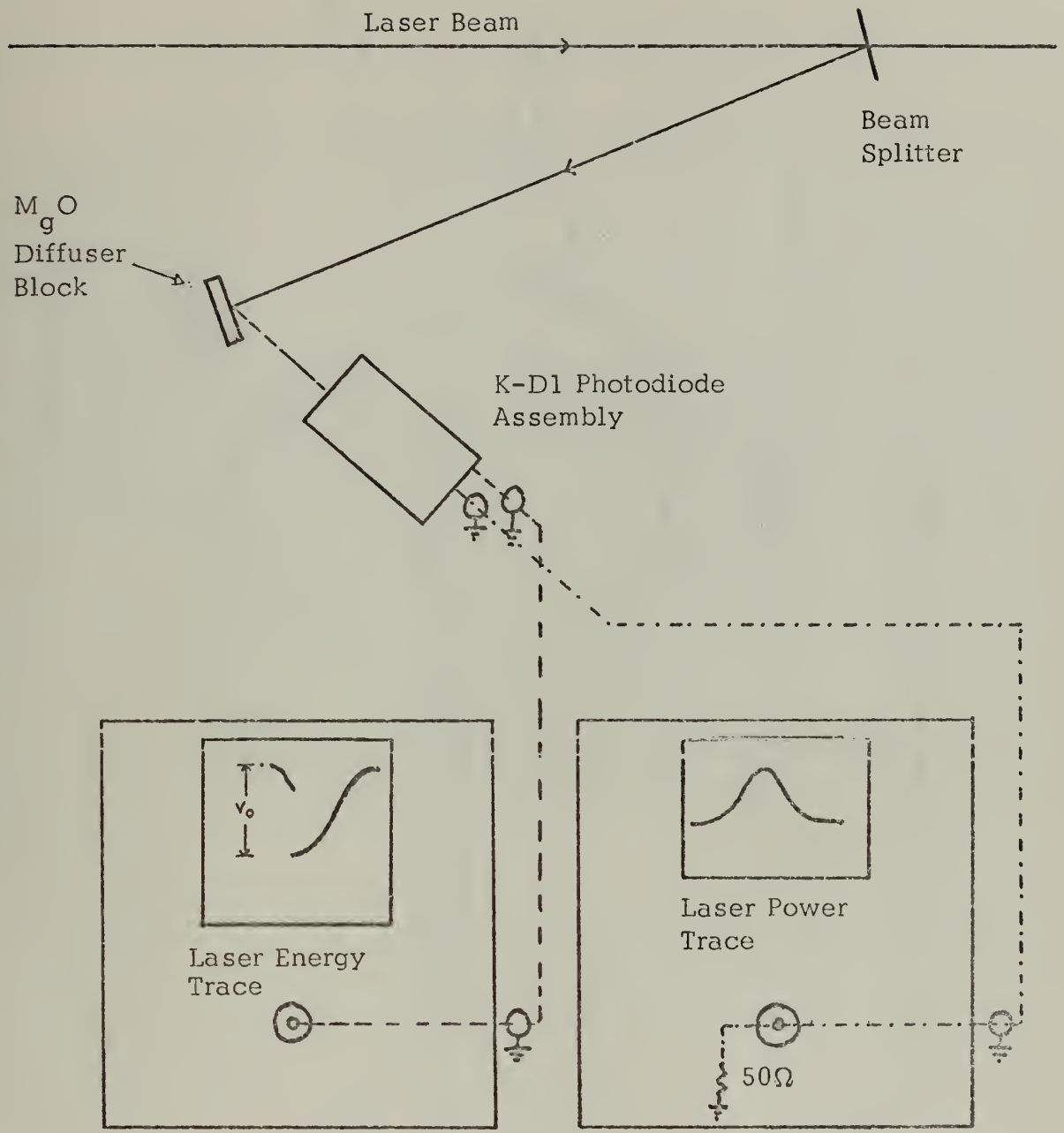

Fig. 6. K-D1 Photodiode Monitoring Configuration

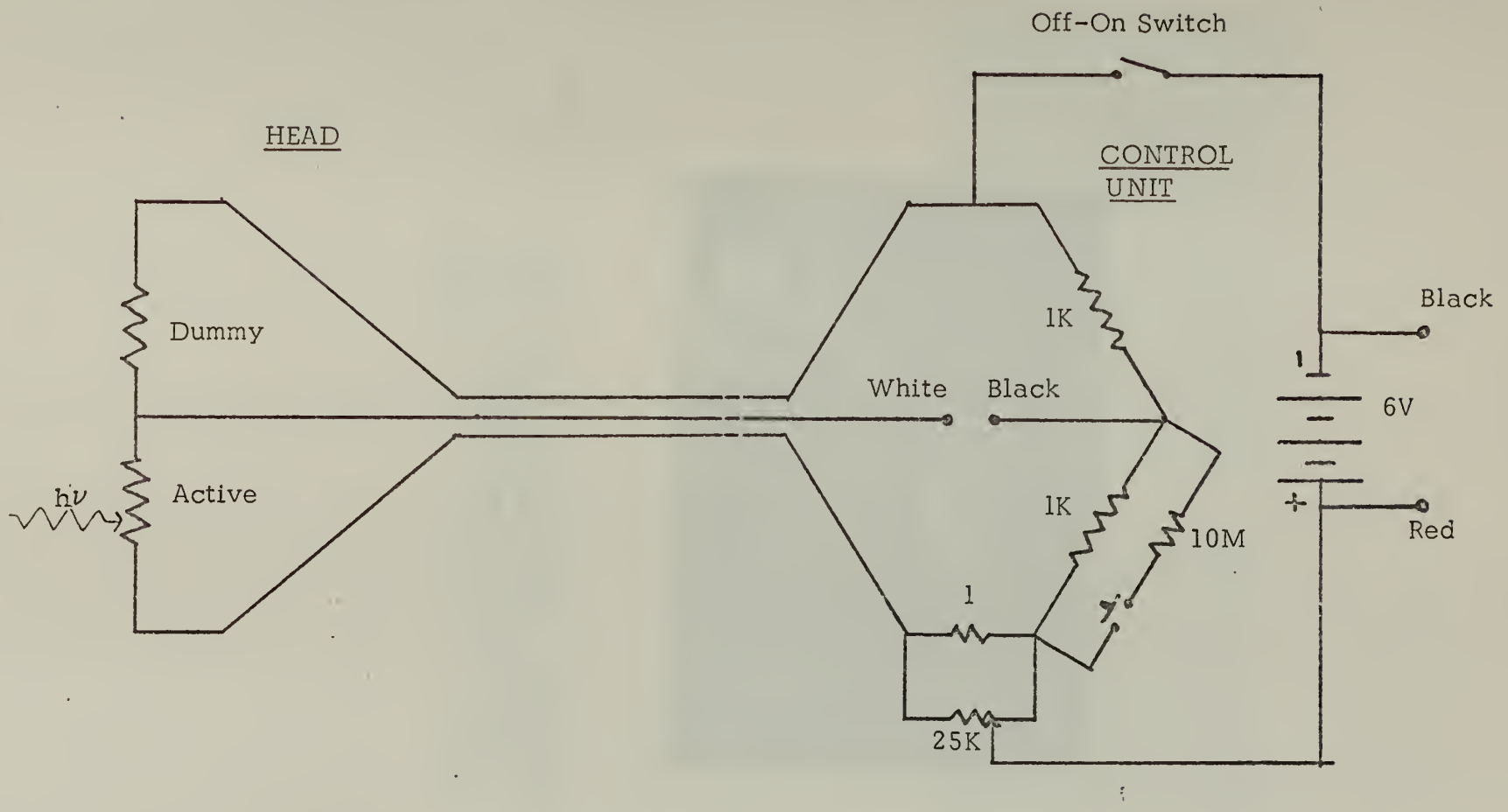

Fig. 7. RN-1 Radiometer Circuit Diagram

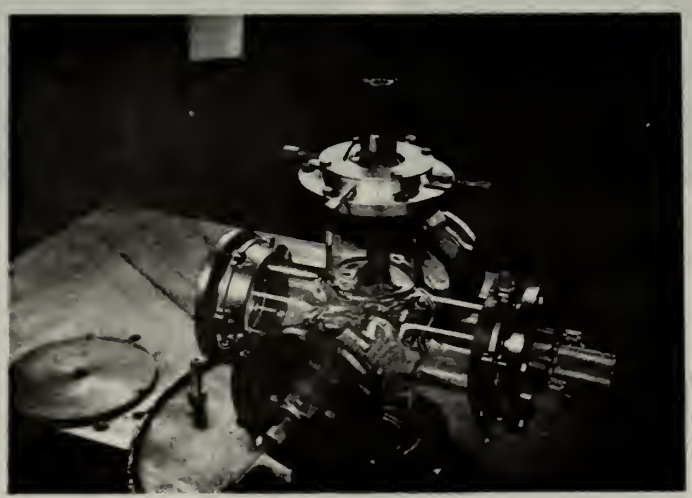

Fig. 8. Four-Port Vacuum Chamber w/Focusing Lens. Laser beam incident from right. Top port used for adjustable target holder. Near port used for insertion of magnetic coil probes.

(a) (b)

Fig. 9. Laser Power Traces. (a) without target (MYLAR film) in place, (b) with target in position. Scale: 5 ns/div.

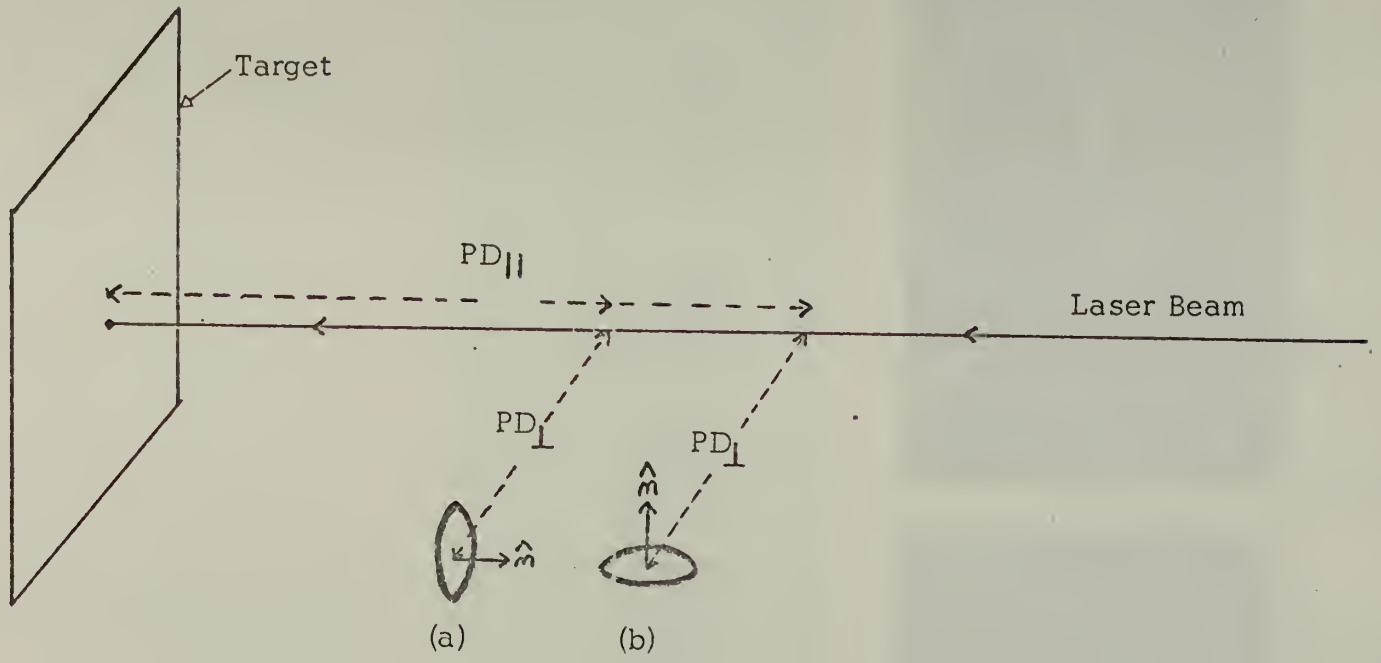

Fig. 10. Description of Magnetic Probe Orientations and Positions. $PD_{||}$ is the distance from the focal spot to the center of the probe along the beam direction. $PD_{\perp}$ is the distance from the incident beam to probe center. (a) and (b) show the probe orientations; ($||$) and ($\perp$), respectively.

(a) (b)

Fig. 11. Magnetic Probe Signals with Reversed Probe Orientations. (a) Large (1 cm dia.) probe in ($\perp$) orientation, (b) same probe rotated by 180°.

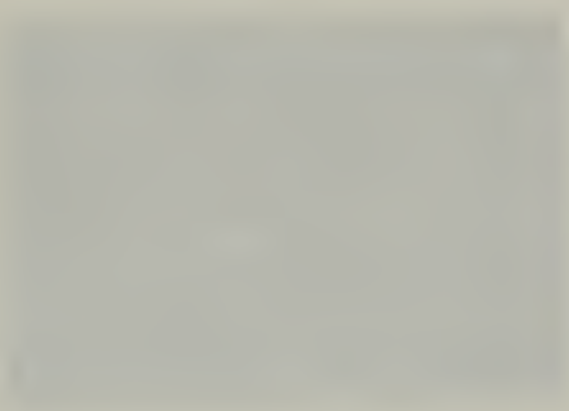

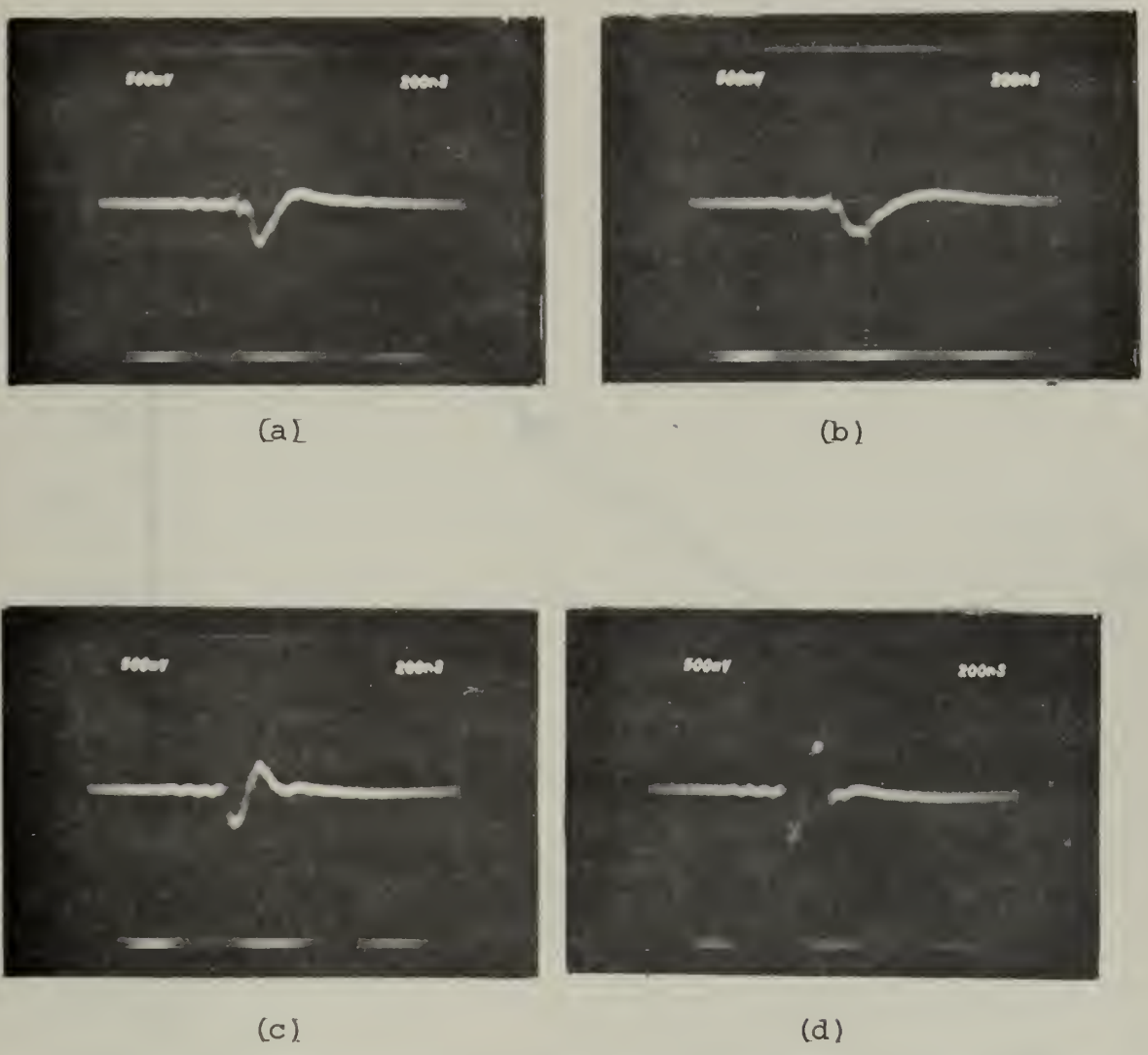

Fig. 12. Magnetic Probe Signals at Various Background Gas Pressures. $PD_{\parallel}$ = 0.60 cm. $PD_{\perp}$ = 0.60 cm probe orientation = ($\perp$). (a) $6.0 \cdot 10^{-4}$ Torr, (b) 1.0 micron, (c) 200 micron, (d) 350 micron. Backround gas - N_2. The magnitudes of the SGMF may be estimated by the absolute area under the curve.

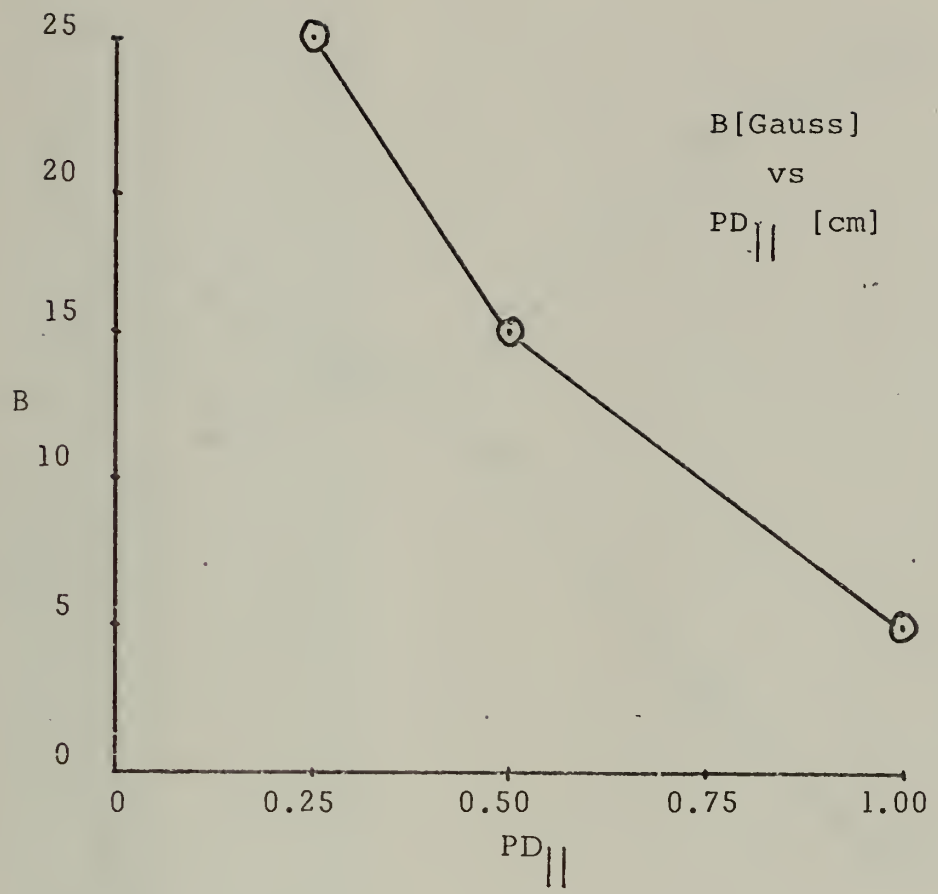

Fig. 13. Variation of SGMF with Respect to Parallel Probe Position. $PD_{\perp}$ = 0.25 cm. Background pressure = 50 microns N_2. All measurements were taken with magnetic coil probe in the perpendicular ($\perp$) orientation. Small 10 turn probe used for measurement.

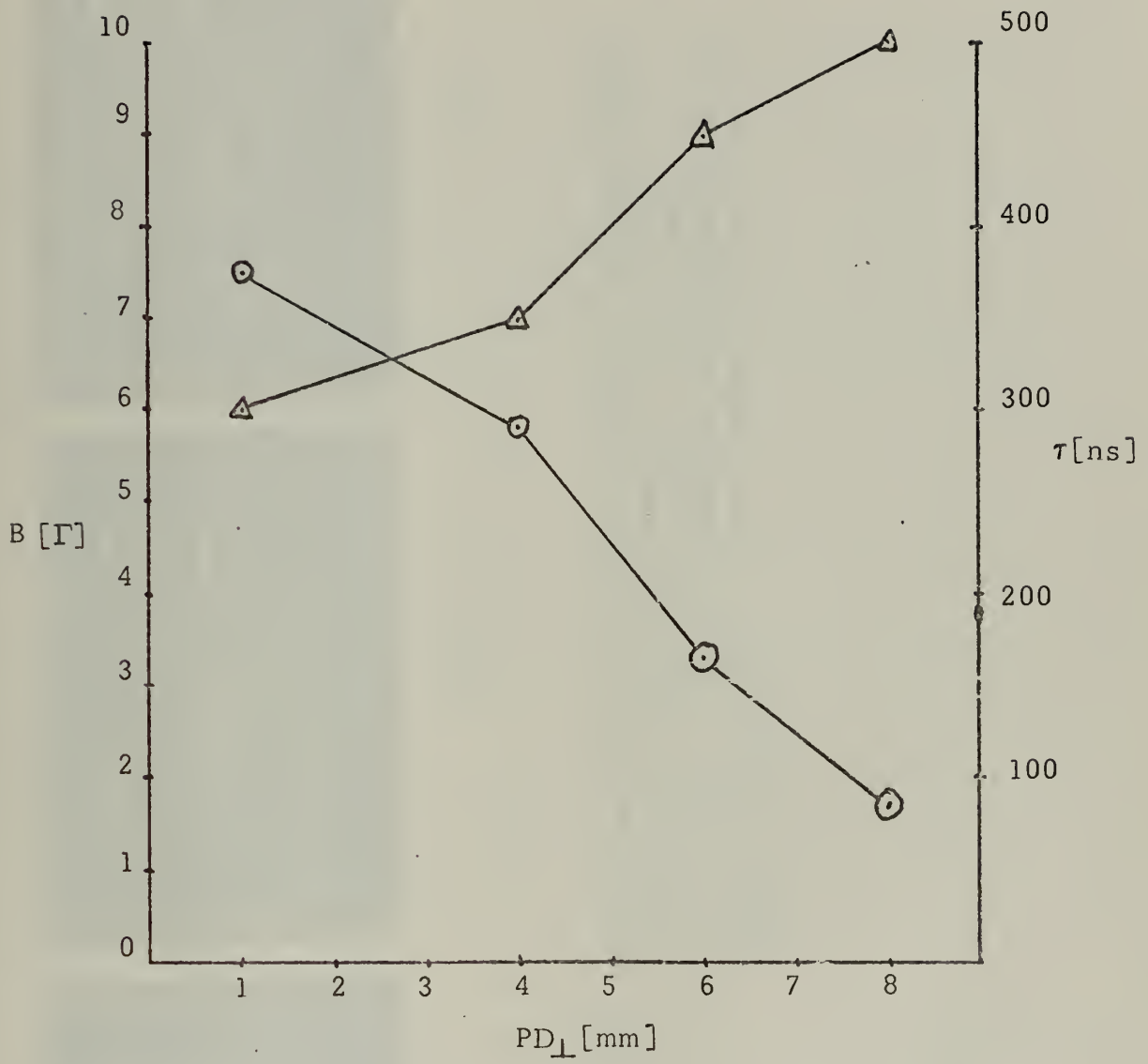

Fig. 14. Variation of SGMF with Respect to Perpendicular Probe Position ($PD_{\perp}$). $PD_{\parallel}$ = 0.75 cm. Background pressure = 65 microns of N_2.
Δ = τ [ns]; θ = B[Gauss].

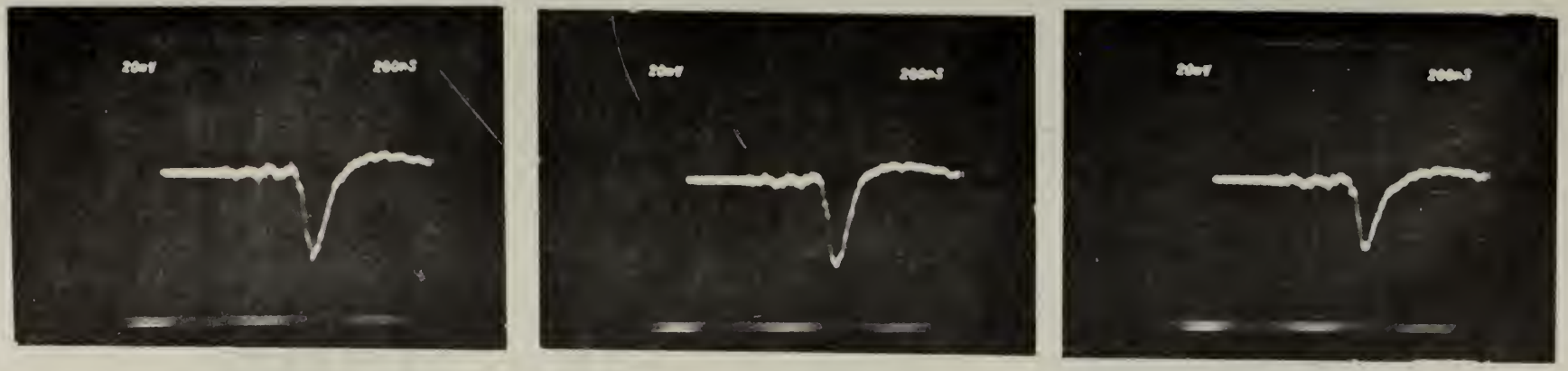

(a) (b) (c)

Fig. 15. Integrated Magnetic Probe Signals at Various Values of Externally Applied Magnetic Field Perpendicular to the Laser Beam, (a) 0 Gauss, (b) 21 Gauss, (c) 43 Gauss. Slight anomalies are probably due to target orientation. Time constant [integrating circuit] ~$3(10^{-7})$ sec.

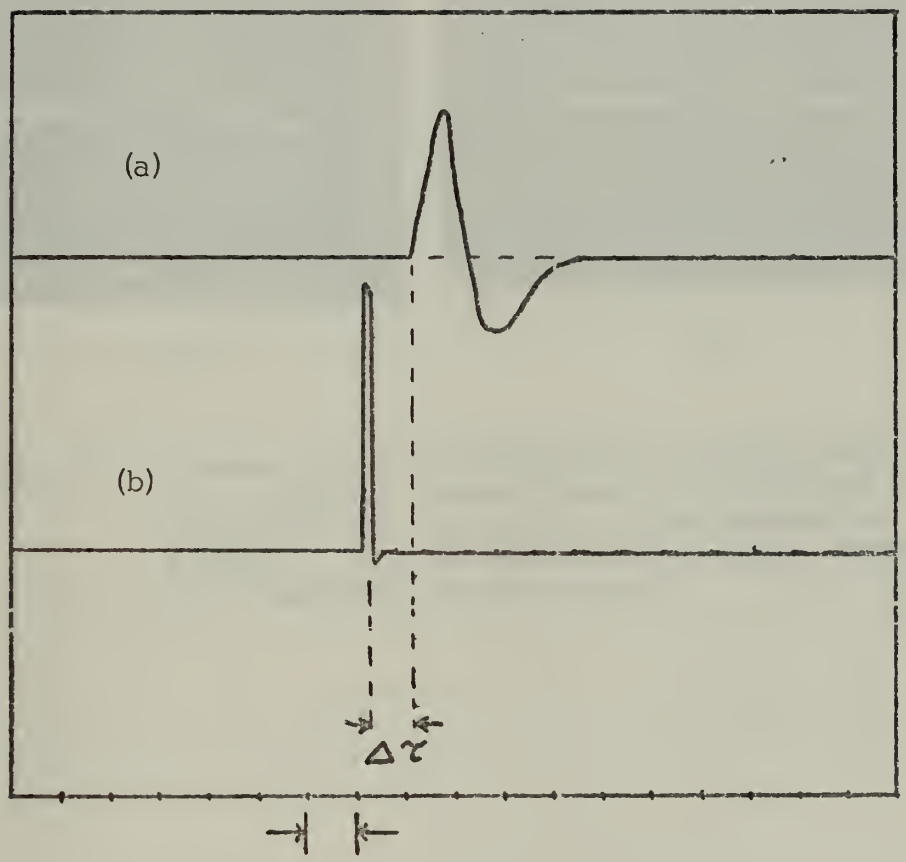

Fig. 16. Typical Oscilloscope Trace for Determination of Magnetic Field Propagation Velocity. Trace (a) is the magnetic probe signal, trace (b) is the laser power signal. Both sweeps are triggered simultaneously by t-OUT which corresponds to application of Pockels cell bias voltage. time scale: 100 ns/div.

(a) (b)

Fig. 17. Comparison of Electrostatic Probe Signal and Magnetic Probe Signal with Probes Colocated in the Path of the Expanding Plasma. (a) Electrostatic probe signal, (b) Magnetic Probe signal.

LIST OF REFERENCES

1. Demtroder, W. and Jantz, W., "Investigation of Laser-produced Plasmas from Metal Surfaces," Plasma Physics, v. 12, pp. 691-703, December 1970.

2. Dawson, J. M., "On the Production of Plasma by Giant Pulse Lasers," The Physics of Fluids, v. 7, pp. 981-987, July 1964.

3. Afanas'ev, Y. V. and Krokhin, O. N., "Vaporization of Matter Exposed to Laser Emission," Soviet Physics JETP, v. 25, no. 4, pp. 639-645, October 1967.

4. Fader, W. J., "Hydrodynamic Model of a Spherical Plasma Produced by Q-Spoiled Laser Irradiation of a Solid Particle," The Physics of Fluids, v. 11, no. 10, pp. 2200-2208, October 1968.

5. Steinhauer, L. C. and Ahlstrom, H. G., "One-Dimensional Laser Heating of a Stationary Plasma," The Physics of Fluids, v. 14, no. 1, pp. 81-93, January 1971.

6. Dawson, J., Kaw, P., and Green, B., "Optical Absorption and Expansion of Laser-produced Plasmas," The Physics of Fluids, v. 12, no. 4, pp. 875-882, April 1969.

7. Korobkin, V. N. and Serov, R. V., "Investigation of the Magnetic Field of a Spark Produced by Focusing Laser Radiation," ZhETF Pis'ma, v. 4, no. 3, pp. 103-106, August 1966.

8. Askar'yan, G. A., and others, "Currents Produced by Light Pressure when a Laser Beam Acts on Matter," ZhETF Pis'ma, v. 5, no. 4, pp. 116-118, February 1967.

9. Stamper, J. A., and others, "Spontaneous Magnetic Fields in Laser-produced Plasmas," Physical Review Letters, v. 26, no. 17, pp. 1012-1015, April 1971.

10. Laser Technology and Applications, Marshall, S. L., ed, p. 65, McGraw-Hill, 1968.

11. Schadegg, L. M., The Dynamics of a Laser-produced Heavy Ion Plasma, MS Thesis, Naval Postgraduate School, Monterey, 1970.

12. Glasstone, S. and Lovberg, R. H., Controlled Thermonuclear Reactions, p. 202, D. Van Nostrand Company, 1960.

13. Shearer, J. W., "Effect of Oblique Incidence on Optical Absorption of Laser Light by a Plasma," The Physics of Fluids, v. 14, no. 1, pp. 183-185, January 1971.

14. Basov, N. G., and others, "High Temperature Effects of Intense Laser Emission Focused on a Solid Target," Soviet Physics JETP, v. 27, no. 4, pp. 575-582, October 1968.

15. Vainshtein, S. J., "The Generation of a Large-scale Magnetic Field by a Turbulent Fluid," Soviet Physics JETP, V. 31, no. 1, pp. 87-89, July 1970.

16. Moffatt, H. K., "Dynamo Action Associated with Random Inertial Waves in a Rotating Conducting Fluid," J. Fluid Mechanics, v. 44, part 4, pp. 705-719, 1970.

17. Hora, H. and Wilhelm, H., "Optical Constants of Fully Ionized Hydrogen Plasma for Laser Radiation," Nuclear Fusion, v. 10, pp. 111-116, 1970.

18. Lindl, J. D. and Kaw, P. K., "Pondermotive Force on Laser-produced Plasmas," The Physics of Fluids, v. 14 no. 2, pp. 371-377, February 1971.

19. Kubo, H., Kawashima, N., and Itoh, T., "Interaction of Plasma Streams with a Neutral Gas Cloud," Plasma Physics, v. 13, pp. 131-140, January 1971

20. Basov, N. G., and others, "Heating and Decay of Plasma Produced by a Giant Laser Pulse Focused on a Solid Target," Soviet Physics JETP, v. 24, no. 4, pp. 659-666, April 1967.

21. Tuckfield, R. G . and Schwirzke, F., "Dynamics of a Laser Created Plasma Expanding in a Magnetic Field," Plasma Physics, v. 11, pp. 11-18, 1969.

22. Schwirzke, F., "Investigation of Laser Produced Plasmas in a Magnetic Field," paper presented at Fourth European Conference on Controlled Fusion and Plasma Physics, Rome, Italy, 31 August-4 September 1970.

INITIAL DISTRIBUTION LIST

		No. Copies
1.	Defense Documentation Center Cameron Station Alexandria, Virginia 22314	2
2.	Library, Code 0212 Naval Postgraduate School Monterey, California 93940	2
3.	Professor Fred Schwirzke, Code 61Sw Department of Physics Naval Postgraduate School Monterey, California 93940	5
4.	CPT Larry J. Davis, USA USA Ordnance Center and School Class Number 4-9-C22, #31 Aberdeen Proving Grounds, Maryland 21005	1

UNCLASSIFIED

Security Classification

DOCUMENT CONTROL DATA - R & D

(Security classification of title, body of abstract and indexing annotation must be entered when the overall report is classified)

ORIGINATING ACTIVITY (Corporate author)

Naval Postgraduate School
Monterey, California 93940

2a. REPORT SECURITY CLASSIFICATION

Unclassified

2b. GROUP

3. REPORT TITLE

Self-generated Magnetic Fields Produced by Laser Bombardment of a Solid Target

4. DESCRIPTIVE NOTES (Type of report and, inclusive dates)

Master's Thesis; June 1971

5. AUTHOR(S) (First name, middle initial, last name)

Larry Joe Davis

6. REPORT DATE	7a. TOTAL NO. OF PAGES	7b. NO. OF REFS
June 1971	71	22

8a. CONTRACT OR GRANT NO.	9a. ORIGINATOR'S REPORT NUMBER(S)
b. PROJECT NO.	
c.	9b. OTHER REPORT NO(S) (Any other numbers that may be assigned this report)
d.	

10. DISTRIBUTION STATEMENT

Approved for public release; distribution unlimited.

11. SUPPLEMENTARY NOTES	12. SPONSORING MILITARY ACTIVITY
	Naval Postgraduate School Monterey, California 93940

13. ABSTRACT

To investigate the phenomena associated with the production of dense plasmas through solid target bombardment by focused laser radiation, procedures relevant to assembly and operation of a high power giant pulse laser system, laser monitoring techniques, and the experimental arrangement for investigating the properties of a freely expanding plasma were developed.

Using magnetic coil probes in the vicinity of the expanding laser-created plasma, signals were detected which indicated the presence of azimuthal magnetic fields. The magnitudes of the observed magnetic fields were as high as 35 Gauss. The dependencies of the self-generated magnetic fields (SGMF) upon background gas pressure, probe position, and applied external fields were investigated.

A discussion of possible generation mechanisms in light of the experimental evidence is included.

DD FORM 1 NOV 65 1473 (PAGE 1)

S/N 0101-807-6811

UNCLASSIFIED

Security Classification

KEY WORDS	LINK A		LINK B		LINK C	
	ROLE	WT	ROLE	WT	ROLE	WT
elf-generated Magnetic Fields						
agnetic Probe Signal						
lectro-optical Shutter						
scillator-amplifier Laser System						
DP (Potassium Dihydrogen Phosphate)						
ropagation Velocity						
lectrostatic Probe Signal						
yrotropic Turbulence						
hermo-electric Junction						

Thesis
D1716 Davis
c.1
128622
Self-generated magnetic fields produced by laser bombardment of a solid target.